Communications

Selective Catalysis of the Aerobic Oxidation of Cyclohexane in the Liquid Phase by Carbon Nanotubes**

Hao Yu, Feng Peng,* Jun Tan, Xiaowei Hu, Hongjuan Wang, Jian Yang, and Wenxu Zheng

The selective oxidation of cyclohexane (C_6H_{12}) is extremely important in the chemical industry, because it produces a series of useful chemicals, including cyclohexanone ($C_6H_{10}(=O)$), cyclohexanol ($C_6H_{11}OH$), and organic acids such as adipic acid (AA).[1] The biggest challenge of commercial processes is the difficulty in controlling the selectivity to target products. For example, to obtain KA oil (a mixture of $C_6H_{10}(=O)$ and $C_6H_{11}OH$), a low conversion of less than 5% is preferentially required by preventing the deep oxidation to by-products. In contrast, adipic acid is normally produced through oxidation of KA oil by HNO_3, causing large energy consumption and emission of nitric oxides.[2] The direct conversion of cyclohexane into adipic acid would be an extremely useful route.[3] However, its application is still hindered by inferior activity and safety issues, despite considerable efforts to optimize the working parameters.

Transition-metal salts containing Co^{2+}, Cr^{2+}, or Mn^{2+} and metalloporphyrins[4] have been used to catalyze cyclohexane oxidation. They can accelerate the initiation of the free radical chain reaction by participating in a Haber–Weiss cycle.[5] The major disadvantage of homogeneous catalysts is the difficulty of catalyst recycling. Moreover, carboxylate groups from the catalyst and degradation species trigger serious pipeline fouling. Solid systems such as zeolites,[6] supported metal catalysts,[7] and metal–organic framework immobilized metalloporphyrin[8] have been reported to be active. Recently, Wang et al. reported that B,N-doped carbon materials can catalyze the oxidation of cyclohexane with H_2O_2 as oxidizing agent.[9] We herein demonstrate that carbon nanotubes (CNTs), as a new class of metal-free catalyst, can afford an excellent activity in the aerobic oxidation of cyclohexane. Under similar conditions, CNTs displayed a

reaction rate 2–10 times higher than those of Au/ZSM-5[7b] and FeAlPO[6c] catalysts. When nitrogen atoms are used to dope graphitic domains, the whole reaction can be altered to one-step production of adipic acid to give selectivities as high as 60% at a conversion higher than 40%.

Catalytic performances of carbon materials, including activated carbon (AC), multiwalled CNTs, and typical metal catalysts are summarized in Table 1. As expected, the blank experiment without any catalyst gives a C_6H_{12} conversion of 6.1% after a reaction time of 8 h, as a result of the autoxidation reaction.[10] The ketone/alcohol (K/A) ratio of approximately 1:1 in the blank experiment agrees with the noncatalytic mechanism of C_6H_{12} oxidation, in which $C_6H_{10}(=O)$ and $C_6H_{11}OH$ are produced equimolarly through decomposition of cyclohexyl hydroperoxide ($C_6H_{11}OOH$). Carbon materials are active for the C_6H_{12} oxidation. High activity was obtained over CNTs to yield a conversion of 34.3%, which is remarkably higher than those on AC, supported Au, and FeAlPO catalysts.

A trace amount of residual iron was reported to improve significantly the catalytic property of CNTs for certain processes.[11] To eliminate its influence on our reaction data, 4.2% Fe_2O_3 was loaded on the CNTs that were thoroughly washed with hydrochloric acid. As shown in Figure S1 (Supporting Information), there was no obvious change in cyclohexane conversion, indicating that iron does not participate in the metal-free reaction.

Since heteroatom doping can be an effective way to enhance the performance of carbon materials, nitrogen-doped CNTs were synthesized by chemical vapor deposition with aniline as both carbon and nitrogen source. The growth of N-doped CNTs was carried out in NH_3 atmosphere to increase the N content and the proportion of pyridinic nitrogen (Figure S2 in the Supporting Information), which may be responsible for the activity of N-doped carbon.[12] After purification with HCl, the N-doped CNTs (Figure 1a,b) possess an N/C atomic ratio of 4.5% as detected by X-ray photoelectron spectroscopy and a similar BET surface area to the undoped CNTs, that is, 155.1 m^2g^{-1}. The residual Fe content was 1.3 wt% in the bulk and lower than the detection limits of XPS on the surface, indicating that the effect of residual catalyst can be ignored. The typical morphology of N-doped CNTs with compartments in bamboolike nanofilaments was observed.[13] The N 1s spectrum in Figure 1c shows a bimodal shape with peaks at 398.3 and 400.8 eV, thus demonstrating the co-existence of 34% sp^2-hybridized pyridinic nitrogen and 66% embedded nitrogen in graphene sheets.[14]

Both undoped CNTs and N-doped CNTs were evaluated under similar reaction conditions. The initial reaction rates of

[*] Prof. H. Yu, Prof. F. Peng, J. Tan, X. W. Hu, Prof. H. J. Wang,
Prof. J. Yang
School of Chemistry and Chemical Engineering
South China University of Technology
Guangzhou, Guangdong, 510640 (China)
Fax: (+86) 20-8711-4916
E-mail: cefpeng@scut.edu.cn

Prof. W. X. Zheng
Department of Applied Chemistry, College of Science
South China Agricultural University
Guangzhou, Guangdong, 510640 (China)

Supporting information for this article is available on the WWW
under http://dx.doi.org/10.1002/anie.201007932.

© 2011 Wiley-VCH Verlag GmbH & Co. KGaA, Weinheim

Table 1: BET specific surface areas and performance of carbon materials in cyclohexane aerobic oxidation.[a]

Catalyst	S_{BET} [m^2 g^{-1}]	X[b] [%]	r_W[c] [mmol g^{-1} h^{-1}]	r_S[d] [mmol m^{-2} h^{-1}]	Selectivity[e] [%]		K/A
					KA	AA	
CNT	127.8	34.3	373	2.9	40.4	52.4	1.2
CNT[f]	–	32.0	–	–	40.0	52.8	1.4
N-CNT	155.1	45.3	879	5.7	26.7	59.7	1.1
AC	1187	15.5	111	0.09	44.5	55.5	0.6
blank[g]	–	6.1	–	–	63.9	21.3	0.95
Au/ZSM5[h]	421	15	185	–	92	n.d.	2.8
FeAlPO[i]	–	3.9	31	–	12.5	53.7	–[j]

[a] Conditions: 398 K, 1.5 MPa O$_2$, 93.6 g C$_6$H$_{12}$, 2.6 g C$_6$H$_{10}$O, 64 g acetone, 16.2 g butanone, 200 mg catalyst. [b] C$_6$H$_{12}$ conversion at 8 h. [c] Initial rate of C$_6$H$_{12}$ consumption per gram of catalyst. [d] Initial rate of C$_6$H$_{12}$ consumption per m^2 of catalyst surface. [e] Selectivity of major products at 8 h. The by-products include C$_6$H$_{11}$OOH, glutaric acid, and succinic acid. [f] Recycled for the third time. [g] Without catalyst. [h] Ref. [7b]: 423 K, 1 MPa O$_2$, 3 h. [i] Ref. [6c]: 403 K, 1.5 MPa air, 8 h. [j] No C$_6$H$_{11}$OH detected.
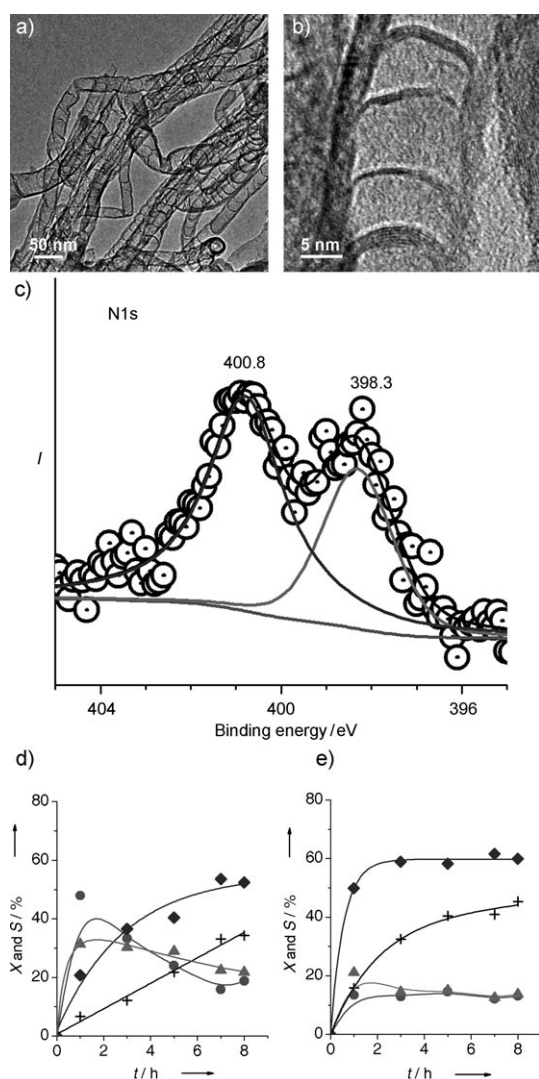

Figure 1. a) Low- and b) high-magnification TEM images of N-doped CNTs. c) XPS N 1s spectrum of N-doped CNTs; ○ experimental data, —— Shirley background and deconvolution of experimental data. d,e) Activity and selectivity of d) undoped and e) N-doped CNTs in aerobic liquid-phase oxidation of C$_6$H$_{12}$. Conditions: 398 K, 1.5 MPa O$_2$, 93.6 g C$_6$H$_{12}$, 2.6 g C$_6$H$_{10}$(=O), 64 g acetone, 16.2 g butanone, 200 mg CNTs. + C$_6$H$_{12}$ conversion, ● C$_6$H$_{11}$OH selectivity, ▲ C$_6$H$_{10}$(=O) selectivity, ◆ AA selectivity.

N-doped CNTs, normalized by catalyst weight and BET surface area, were 2.4 and 2 times as high as those of the undoped CNTs, respectively. As seen in Figure 1d,e, the doped sample displays an enhanced activity and a higher selectivity to adipic acid. As we analyzed the reaction profiles, we found the conversion to adipic acid was significantly accelerated in the very beginning of the reaction. After 1 h, the selectivity to adipic acid reached 50%, which is 2.5 times higher than that on the undoped sample at the same stage. Along with the reaction time, 59.7% AA and 26.7% KA oil selectivity with a K/A ratio (ratio of C$_6$H$_{10}$(=O) yield to C$_6$H$_{11}$OH yield) of 1.1 was achieved at a conversion of 45.3%. Considering the lack of an optimized structure and composition at present, we believe that there are still many possibilities to enhance the performance of N-doped CNTs.

The N-doped CNT catalyst also shows desired recyclability. During five cycling tests, there is almost no difference in both relative activity (defined as the conversion after 8 h reaction normalized by that of the first run, RA) and AA and KA oil selectivity (Figure 2). The K/A ratios are always around 0.8 to 1.2. The stable catalytic performance of N-doped CNTs indicates that the active domains of N-doped CNTs are stable during the turnover of C$_6$H$_{12}$ and formation of organic acid, ketone, and alcohol.

To our knowledge, the activity of N-doped CNT is higher than that of most of the solid catalysts reported, such as supported nanogold and zeolites. Dugal et al.[6c] designed a
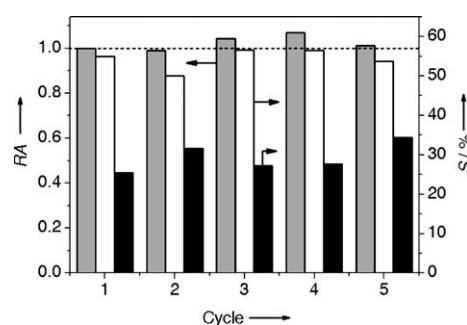

Figure 2. Recyclability of N-doped CNTs in liquid-phase cyclohexane oxidation. Conditions: 398 K, 1.5 MPa O$_2$, 93.6 g C$_6$H$_{12}$, 2.6 g C$_6$H$_{10}$(=O), 64 g acetone, 16.2 g butanone, 200 mg catalyst, 8 h. Gray column: RA, white column: AA selectivity, and black column: selectivity of KA oil.

Fe^{III}-substituted aluminium phosphate with properly tailored pore size to facilitate the formation of AA in pores. Compared with FeAlPO, CNTs and N-doped CNTs have similar AA selectivity, but lower selectivity of decarboxylated by-products. Because no metal is involved, carbon-catalyzed C_6H_{12} oxidation is low-cost, the catalyst is easy to recover, and the reaction is resistant against pipeline fouling. Owing to their high activity, controllable selectivity, and outstanding recyclability, CNTs are promising catalysts for cyclohexane conversion as well as single-step production of adipic acid.

It is widely accepted that the liquid-phase oxidation of C_6H_{12} proceeds through a radical-involved autoxidation process.[10b,c] The product cyclohexanone (C_6H_{10}(=O)) can also catalyze the initiation of a chain reaction [Eq. (1)].[10a]

$$C_6H_{11}OOH + C_6H_{10}(=O) \rightarrow C_6H_{11}O^{\cdot} + {}^{\cdot}C_6H_9(=O)\,(-\alpha H) + H_2O \tag{1}$$
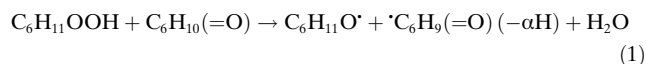
To prove the dominant role of radical species in our system, p-benzoquinone as a typical radical scavenger was added to the reactor. As shown in Table 2, the reaction was almost totally suppressed to give a conversion as low as 0.8% with the addition of p-benzoquinone. Similar to the reported catalysts,[10a] a positive effect of cyclohexanone product was also observed. With its presence, the conversion was elevated from 14.0 to 21.8%. The apparent activation energy (E_a) was calculated from the reaction data (Figure S3 in the Supporting Information). The overall E_a value for cyclohexane conversion is (111.5 ± 15.5) kJ mol^{-1}, which is extremely close to the value for Equation (1), that is, in the autoxidation of cyclohexane, calculated by transition-state theory $(116.3$ kJ mol$^{-1})$.[10a,15] A similar reaction mechanism was then proved for our CNT-based process. The E_a values of the oxidation with cyclohexanol and cyclohexanone as starting materials were (37.5 ± 6.2) and (41.7 ± 5.1) kJ mol^{-1}, respectively, showing that the chain initiation is probably the rate-determining step. It should be emphasized that the catalytic role of CNTs in the C_6H_{12} oxidation is crucial. Even without the C_6H_{10}(=O) initiator, CNTs were an effective catalyst for the aerobic oxidation of C_6H_{12}.

Diverse catalytic properties of CNTs have been reported, including the activation of hydrocarbon,[16] oxygen,[17] and hydrogen[18] molecules. Electron-donating nitrogen species at the exposed graphitic defects were reported to facilitate the adsorption of reactive intermediates and thus improve the electrocatalysis of oxygen reduction.[19] Discussions on the mechanism of liquid-phase processes can be found in only a few works. The kinetics for the radical autoxidation was shown to relate to the chain length of radical reaction.[10a] Also, CNTs were found to accelerate the electron-transfer induced decomposition of radical precursors, including organic peroxides.[20] The CNTs are expected to accept and stabilize the radicals by forming new intermediates, which are able to abstract hydrogen atoms from cyclohexane. An improved lifetime with respect to that of peroxyl radicals is probably assured by the large π system of graphitic units, especially in the presence of N-containing complexes.[21] This phenomenon can be evidenced by the unchanged I_D/I_G ratio in the Raman spectra during recycling of CNT catalysts over three cycles as an important indicator of the extent of ordering of carbon materials (Figure S4 in the Supporting Information). Results from transmission infrared spectroscopy and surface functionality analysis by Boehm titration also show almost the same surface properties before and after reaction (Figures S5 and S6 in the Supporting Information). The stabilization of peroxyl radicals by π–π conjugation between radical and CNTs is also supported by a theoretical calculation performed at the B3LYP level of DFT theory. Our calculations have revealed that the $C_6H_{11}OO^{\cdot}$ radical, the most important intermediate in the oxidation of cyclohexane, can form a π–π stacking complex with a CNT or N-doped CNT (represented by a nitrogen atom embedded in a graphene sheet), as the optimized structures shown in Figure 3. The radical is approximately 3.9 Å away from the CNT and approximately 3.5 Å away from the N-doped CNT. The energy of the interaction between the two species was calculated to be 6.1 kJ mol^{-1} for the radical CNT complex and 60.3 kJ mol^{-1} for the radical N-doped CNT complex. These results imply that the radical can be stabilized by the CNT and N-doped CNT. Moreover, the radical N-doped CNT complex is much more stable than the radical CNT complex, which is consistent with the higher activity of N-doped CNT.

Studies on the gas-phase reaction show the crucial role of surface functionalities in the catalytic performance of CNTs.[16a,22] For example, in the oxidative dehydrogenation reactions, the Lewis basic C=O sites are responsible for activating hydrocarbons, while the graphene plane may dissociate oxygen molecules.[16a,c,17] As shown in Table 3, in contrast, there is a negative effect for the oxygen functionalities on the activity of C_6H_{12} oxidation. It was also shown that this negative effect of groups on the activity did not originate from the weaker adsorption of C_6H_{12} on the hydrophilic surface of oxidized CNTs (Figure S7 in the Supporting Information). Such an effect is probably caused by the localization of electrons as a result of the introduction of groups and defects, which may be adverse to the π–π interaction between the radical and graphene planes and is supported by the catalytic performance of CNTs annealed at high temperatures (Table 3). The annealing of CNTs can decompose the oxygenous groups and benefit the repair of the defects, indicated by the decrease of I_D/I_G ratios with annealing temperature. The conversion of C_6H_{12} increased with annealing temperature, indicating that CNTs with higher long-range order and electron delocalization are preferred. Thus, the introduction of electron-donating nitrogen species

Table 2: Effect of C_6H_{10}(=O), CNTs, and p-benzoquinone radical scavenger on the C_6H_{12} conversion.[a]

Entry	C_6H_{10}(=O)[b]	CNTs[b]	p-benzoquinone	X[c] [%]
1	○	×	×	2.6
2	×	○	×	14.0
3	○	○	×	21.8
4	○	○	○	0.8

[a] Conditions: 398 K, 1.5 MPa O_2, 93.6 g C_6H_{12}, 2.6 g C_6H_{10}(=O), 64 g acetone, 16.2 g butanone, 200 mg CNTs, 3 g p-benzoquinone. [b] ○: added; ×: not added. [c] C_6H_{12} conversion at 5 h.
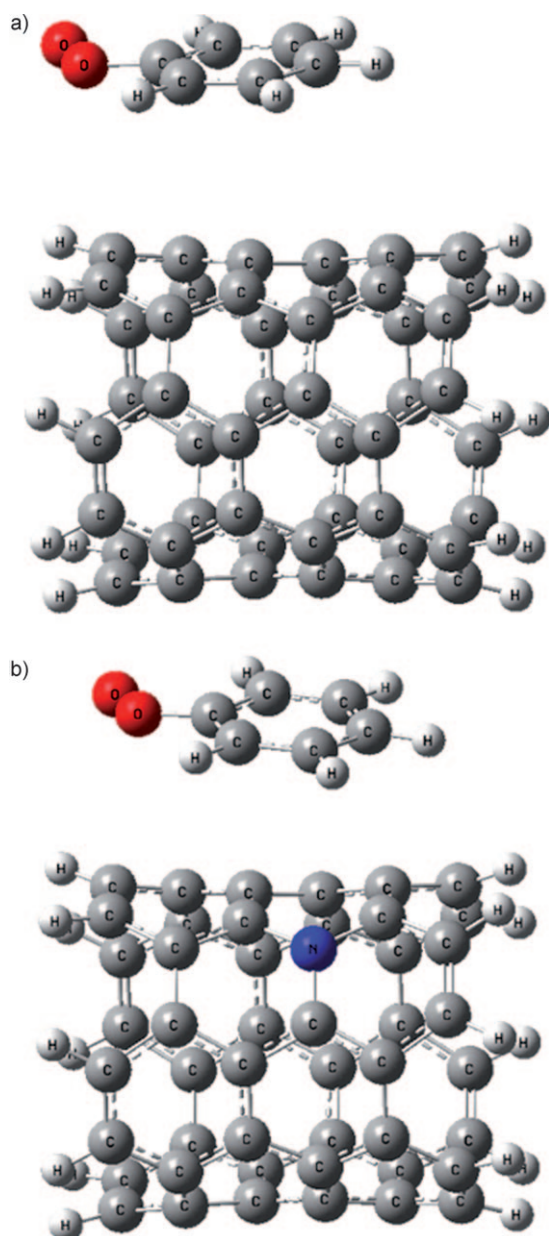
Figure 3. Optimized structures of the supramolecular complexes between a $C_6H_{11}OO\cdot$ radical and a) a CNT and b) an N-doped CNT. Red O, blue N, dark gray C, and light gray H.

in the graphitic domains can further improve the activity, as a result of the enhanced electron transfer.[13a, 23]

In summary, we demonstrated that carbon materials can be used as a metal-free catalyst for the aerobic oxidation of C_6H_{12}. Excellent performance was achieved by using multiwalled CNTs produced by chemical vapor deposition. It should be highlighted that better activity was obtained with as-synthesized CNTs without any posttreatment, which will substantially reduce the cost of a practical catalyst. Electron transfer in graphene sheets plays an important role. Thus, one can further enhance the activity of CNTs by N doping. The results presented herein pave the way for the development of metal-free catalysts for the liquid-phase oxidation of cyclohexane.

Experimental Section

Activated carbon was purchased from Liyang Convoy Activated Carbon Factory. Multiwalled CNTs were produced by the chemical vapor deposition (CVD) method with liquefied petroleum gas as carbon source over a FeMo/Al$_2$O$_3$ catalyst in a horizontal tubular quartz furnace with 4 cm inner diameter (i.d.). Before the growth of CNTs, the catalyst was activated by a mixture of H_2 and N_2 (25 and 25 N cm^{3}min^{-1}) for 30 min. The growth of CNTs was carried out at 700°C for 130 min with 20 N cm^{3}min^{-1} liquefied petroleum gas, 10 N cm^{3}min^{-1} H$_2$, and 50 N cm^{3}min^{-1} N$_2$. The details of catalyst and CNT growth can be found in Ref. [24].

The N-doped CNTs were synthesized by the same CVD method except with aniline as carbon source in NH$_3$ atmosphere. Aniline (10 mL) was injected by a syringe pump at a rate of 3 mLh^{-1} and was vaporized in a quartz tube at 180°C. The flow rate of NH$_3$ was 500 N cm^{3}min^{-1}. The residual FeMo/Al$_2$O$_3$ catalyst was removed by aqueous 12 mol L^{-1} HCl solution. The Fe content of purified sample was measured by atomic adsorption spectroscopy (Shimadazu AAS-6800).

The BET specific surface areas were measured by N$_2$ adsorption at liquid N$_2$ temperature in an ASAP 2010 analyzer. The Raman spectra were obtained in a LabRAM Aramis micro Raman spectrometer with an excitation wavelength at 532 nm with 2 μm spot size. The surface oxygeneous groups were analyzed by Boehm titration.[25] XPS analysis was performed with a Kratos Axis ultra (DLD) spectrometer equipped with an Al$_{K\alpha}$ X-ray source. The binding energies (± 0.2 eV) were referenced to the C$_{1s}$ peak at 284.6 eV. TEM and HRTEM images were obtained with a JEM-2010 microscope operating at 200 kV. Specimens for TEM and HRTEM were prepared by ultrasonically suspending the sample in acetone and depositing a drop of the suspension onto a grid.

Table 3: Properties and performance of the CNTs used in the cyclohexane aerobic oxidation with different HNO$_3$ oxidation durations and annealing temperatures.[a]

Entry	HNO$_3$ reflux[b] [h]	Annealing temperature[c]	S_{BET} [m^{2}g^{-1}]	Raman I_D/I_G[d]	Boehm titration [mmol g^{-1}] -OH	-C=O	-COOH	X[e] [%]	Selectivity[f] [%] KA	AA	K/A
1	0	No[g]	127.8	0.87	0.30	0.18	0.12	34.3	40.4	52.4	1.2
2	0.5	No[g]	130.8	0.98	0.52	0.72	0.33	32.6	33.1	48.5	1.7
3	4	No[g]	136.0	1.06	0.66	1.10	0.55	23.8	36.9	47.5	0.97
4	8	No[g]	149.4	1.16	0.59	1.13	0.97	15.8	39.2	46.7	0.7
5	8	873	–	0.95	–	–	–	20.2	44.5	45.0	1.2
6	8	1173	–	0.92	–	–	–	22.4	32.6	55.5	1.4
7	8	1373	–	0.92	–	–	–	25.8	33.5	47.7	1.0

[a] The reaction was carried out at 398 K, 1.5 MPa O$_2$, and a mass ratio of starting materials of C$_6$H$_{12}$/C$_6$H$_{10}$(=O)/acetone/catalyst = 93.6:2.6:64:0.2. [b] In 9 M HNO$_3$, at 140°C. [c] In Ar gas for 2 h. [d] The excitation wavelength was 532 nm. [e] C$_6$H$_{12}$ conversion at 8 h. [f] Selectivity of major products at 8 h. The by-products include cyclohexyl hydroperoxide, glutaric acid, and succinic acid. [g] Drying in air at 110°C overmight.

Communications

The C_6H_{12} oxidation reaction was carried out in a mechanically stirred 300 mL Parr autoclave in batch mode. Before reaction, reactants with butanone as internal standard, solvent acetone, and catalysts were loaded in the autoclave, and the reactor was flushed with N_2. Then, the reactor was heated to a stable operational temperature, and subsequently pure O_2 was fed into the reactor (defining $t = 0$). The products were analyzed by gas chromatography (GC) and high-performance liquid chromatography (HPLC). GC was used to analyze the concentrations of C_6H_{12}, $C_6H_{11}OH$, and $C_6H_{10}(=O)$ referenced by butanone internal standard. Conditions of GC: DB-5MS capillary column (30 m, DF = 0.25 μm, 0.25 mm i.d.), FID detector, injector temperature 280 °C, and oven temperature 110 °C. A HPLC instrument, equipped with an Agillent Hypersil ODS column (4.6 × 250 mm) and UV detector (at 210 nm), was used to analyze the concentration of AA, glutaric acid, and succinic acid. The eluent was 0.01 mol L^{-1} KH$_2$PO$_4$ in a 1:9 methanol/water mixture.

The structures of the supramolecular complexes between a $C_6H_{11}OO·$ radical and a CNT and an N-doped CNT were fully optimized by analytic gradient techniques. The methods used were density functional theory (DFT) with Becke's three-parameter (B3)[26] exchange functional along with the Lee–Yang–Parr (LYP) nonlocal correlation functional (B3LYP).[27] The standard valence double-ζ basis set augmented with d-type polarization functions and s- and p-type diffuse functions, 6-31 + G (d),[28] was used. Basis set superposition error (BSSE) was corrected for the calculation by applying Boys' and Bernardi's counterpoise procedure (CP).[29] The Gaussian 03 program was used in the calculations.

[1] D. D. Davis in *Ullman's Encyclopedia of Industrial Chemistry*, Vol. A1 (Eds.: W. Gerhartz), Wiley-VCH, Weinheim, **1985**, pp. 269–276.

[2] U. Schuchardt, D. Cardoso, R. Sercheli, R. Pereira, R. S. de Cruz, M. C. Guerreiro, D. Mandelli, E. V. Spinace, E. L. Fires, *Appl. Catal. A* **2001**, *211*, 1–17.

[3] a) E. P. Talsi, V. D. Chinakov, V. P. Babenko, V. N. Sidelnikov, K. I. Zamaraev, *J. Mol. Catal.* **1993**, *81*, 215–233; b) K. Tanaka, *Chem. Technol.* **1974**, *4*, 555–559; c) S. A. Chavan, D. Srinivas, P. Ratnasamyi, *J. Catal.* **2002**, *212*, 39–45; d) K. M. K. Yu, R. Hummeida, A. Abutaki, S. C. Tsang, *Catal. Lett.* **2006**, *111*, 51–55; e) R. Raja, J. M. Thomas, M. C. Xu, K. D. M. Harris, M. Greenhill-Hooper, K. Quill, *Chem. Commun.* **2006**, 448–450.

[4] a) C. C. Guo, M. F. Chu, Q. Liu, Y. Liu, D. C. Guo, X. Q. Liu, *Appl. Catal. A* **2003**, *246*, 303–309; b) B. Y. Hu, Y. J. Yuan, J. Xiao, C. C. Guo, Q. Liu, Z. Tan, Q. H. Li, *J. Porphyrins Phthalocyanines* **2008**, *12*, 27–34; c) C. C. Guo, X. Q. Liu, Y. Liu, Q. Liu, M. F. Chu, X. B. Zhang, *J. Mol. Catal. A* **2003**, *192*, 289–294.

[5] a) R. A. Sheldon, J. K. Kochi, *Metal-Catalyzed Oxidations of Organic Compounds*, Academic Press, New York, **1981**; b) R. P. Houghton, C. R. Rice, *Polyhedron* **1996**, *15*, 1893–1897; c) D. L. Vanoppen, D. E. Devos, M. J. Genet, P. G. Rouxhet, P. A. Jacobs, *Angew. Chem.* **1995**, *107*, 637; *Angew. Chem. Int. Ed. Engl.* **1995**, *34*, 560.

[6] a) J. M. Thomas, R. Raja, G. Sankar, R. G. Bell, *Acc. Chem. Res.* **2001**, *34*, 191–200; b) R. Raja, G. Sankar, J. M. Thomas, *J. Am. Chem. Soc.* **1999**, *121*, 11926–11927; c) M. Dugal, G. Sankar, R. Raja, J. M. Thomas, *Angew. Chem.* **2000**, *112*, 2399–2402; *Angew. Chem. Int. Ed.* **2000**, *39*, 2310–2313; d) E. V. Spinace, H. O. Pastore, U. Schuchardt, *J. Catal.* **1995**, *157*, 631–635.

[7] a) G. M. Lü, R. Zhao, G. Qian, Y. X. Qi, X. L. Wang, J. S. Suo, *Catal. Lett.* **2004**, *97*, 115–118; b) R. Zhao, D. Ji, G. M. Lv, G. Qian, L. Yan, X. L. Wang, J. S. Suo, *Chem. Commun.* **2004**, 904–905; c) A. Ramanathan, M. S. Hamdy, R. Parton, T. Maschmeyer, J. C. Jansen, U. Hanefeld, *Appl. Catal. A* **2009**, *355*, 78–82.

[8] M. H. Alkordi, Y. L. Liu, R. W. Larsen, J. F. Eubank, M. Eddaoudi, *J. Am. Chem. Soc.* **2008**, *130*, 12639–12641.

[9] Y. Wang, J. S. Zhang, X. C. Wang, M. Antonietti, H. R. Li, *Angew. Chem.* **2010**, *122*, 3428–3431; *Angew. Chem. Int. Ed.* **2010**, *49*, 3356–3359.

[10] a) I. Hermans, P. A. Jacobs, J. Peeters, *Chem. Eur. J.* **2006**, *12*, 4229–4240; b) I. Hermans, P. A. Jacobs, J. Peeters, *J. Mol. Catal. A* **2006**, *251*, 221–228; c) I. Hermans, T. L. Nguyen, P. A. Jacobs, J. Peeters, *ChemPhysChem* **2005**, *6*, 637–645.

[11] a) C. E. Banks, A. Crossley, C. Salter, S. J. Wilkins, R. G. Compton, *Angew. Chem.* **2006**, *118*, 2595–2599; *Angew. Chem. Int. Ed.* **2006**, *45*, 2533–2537; b) B. Šljukić, C. E. Banks, R. G. Compton, *Nano Lett.* **2006**, *6*, 1556–1558.

[12] a) S. van Dommele, K. P. de Jong, J. H. Bitter, *Chem. Commun.* **2006**, 4859–4861; b) Y. Y. Shao, J. H. Sui, G. P. Yin, Y. Z. Gao, *Appl. Catal. B* **2008**, *79*, 89–99.

[13] a) P. Ayala, R. Arenal, M. Rummeli, A. Rubio, T. Pichler, *Carbon* **2010**, *48*, 575–586; b) C. J. Lee, S. C. Lyu, H. W. Kim, J. H. Lee, K. I. Cho, *Chem. Phys. Lett.* **2002**, *359*, 115–120; c) B. G. Sumpter, V. Meunier, J. M. Romo-Herrera, E. Cruz-Silva, D. A. Cullen, H. Terrones, D. J. Smith, M. Terrones, *Acs Nano* **2007**, *1*, 369–375.

[14] a) L. S. Panchakarla, A. Govindaraj, C. N. R. Rao, *Acs Nano* **2007**, *1*, 494–500; b) R. Sen, B. C. Satishkumar, A. Govindaraj, K. R. Harikumar, G. Raina, J. P. Zhang, A. K. Cheetham, C. N. R. Rao, *Chem. Phys. Lett.* **1998**, *287*, 671–676.

[15] I. Hermans, J. Peeters, P. A. Jacobs, *Top. Catal.* **2008**, *50*, 124–132.

[16] a) J. Zhang, D. S. Su, A. H. Zhang, D. Wang, R. Schlogl, C. Hebert, *Angew. Chem.* **2007**, *119*, 7460–7464; *Angew. Chem. Int. Ed.* **2007**, *46*, 7319–7323; b) S. Y. Lee, J. H. Kwak, G. Y. Han, T. J. Lee, K. J. Yoon, *Carbon* **2008**, *46*, 342–348; c) J. Zhang, X. Liu, R. Blume, A. H. Zhang, R. Schlogl, D. S. Su, *Science* **2008**, *322*, 73–77.

[17] R. Schlogl, F. Atamny, *Mol. Phys.* **1992**, *76*, 851–886.

[18] B. J. Li, Z. Xu, *J. Am. Chem. Soc.* **2009**, *131*, 16380–19382.

[19] a) K. P. Gong, F. Du, Z. H. Xia, M. Durstock, L. M. Dai, *Science* **2009**, *323*, 760–764; b) R. L. Liu, D. Q. Wu, X. L. Feng, K. Mullen, *Angew. Chem.* **2010**, *122*, 2619–2623; *Angew. Chem. Int. Ed.* **2010**, *49*, 2565–2569.

[20] P. S. Engel, W. E. Billups, D. W. Abmayr, K. Tsvaygboym, R. Wang, *J. Phys. Chem. C* **2008**, *112*, 695–700.

[21] T. Iwahama, K. Syojyo, S. Sakaguchi, Y. Ishii, *Org. Process Res. Dev.* **1998**, *2*, 255–260.

[22] M. F. R. Pereira, J. J. M. Orfao, J. L. Figueiredo, *Appl. Catal. A* **1999**, *184*, 153–160.

[23] a) C. P. Ewels, M. Glerup, *J. Nanosci. Nanotechnol.* **2005**, *5*, 1345–1363; b) C. C. Kaun, B. Larade, H. Mehrez, J. Taylor, H. Guo, *Phys. Rev. B* **2002**, *65*, 205416; c) G. Zhou, W. H. Duan, *J. Nanosci. Nanotechnol.* **2005**, *5*, 1421–1434.

[24] W. Z. Qian, H. Yu, F. Wei, Q. F. Zhang, Z. W. Wang, *Carbon* **2002**, *40*, 2968–2970.

[25] H. P. Boehm, *Carbon* **1994**, *32*, 759–769.

[26] A. D. Becke, *J. Chem. Phys.* **1993**, *98*, 5648–5652.

[27] a) C. Lee, W. Yang, R. G. Parr, *Phys. Rev. B* **1988**, *37*, 785–789; b) B. Miehlich, A. Savin, S. H. , H. Preuss, *Chem. Phys. Lett.* **1989**, *157*, 200–206.

[28] W. J. Hehre, L. Radom, P. R. Schleyer, J. A. Pople, *Ab Initio Molecular Orbital Theory*, Wiley, New York, **1986**.

[29] S. F. Boys, F. Bernardi, *Mol. Phys.* **1970**, *19*, 553–566.